
TPDH-GRAPHENE AS A NEW ANODIC MATERIAL FOR LITHIUM ION BATTERY: DFT-BASED INVESTIGATIONS

Juan Gomez Quispe, Bruno Bueno Ipaves Nascimento, Pedro Alves da Silva Autreto

Center of Natural and Human Sciences, Federal University of ABC

Santo Andre

Sao Paulo, Brazil

pedro.autreto@ufabc.edu.br

Douglas Soares Galvao

galvao@ifi.unicamp.br

Applied Physics Department, State University of Campinas, Campinas, Sao Paulo, Brazil

ABSTRACT

The potential of tetra-penta-deca-hexagonal graphene (TPDH-gr), a recently proposed 2D carbon allotrope as an anodic material in lithium ion batteries (LIB), was investigated through density functional theory (DFT) calculations. The results indicate that Li-atom adsorption is moderate (around 0.70 eV), allowing for easy desorption. Moreover, energy barrier, diffusion coefficient, and open circuit voltage (OCV) calculations show rapid Li atom diffusion on the TPDH-gr surface, stable intercalation of lithium atoms, and good performance during the charge and discharge cycles of the LIB. These findings, combined with the intrinsic metallic nature of TPDH-gr, indicate that this new 2D carbon allotrope is a promising candidate for use as an anodic LIB material.

1 Introduction

Graphene, a revolutionary material, is a two-dimensional (2D) structure composed of a single layer of carbon atoms arranged in a hexagonal honeycomb lattice, where carbon atoms are covalently bonded in sp^2 hybridization [1]. This hybridization results in excellent mechanical rigidity and high electronic mobility due to the sigma and π type bonds [2].

In contrast to graphene, other 2D carbon allotropes can be formed by combining different hybridization states (sp , sp^2 or sp^3) and different types of carbon rings. One example is graphenylene, which is composed of tetragonal (C_4), hexagonal (C_6), and dodecagonal (C_{12}) carbon rings [3]. Calculations based on density functional theory (DFT) indicate that graphenylene has a semiconducting nature with a direct band gap value of approximately 25 meV [4]. Another carbon allotrope, recently synthesized [5], is TPH-graphene, which is formed by C_4 , C_5 , and C_6 carbon rings, which can exist in two different semiconducting phases with direct band gap values of 2.704 and 2.361 eV, respectively [6]. Much of the research related to these new 2D carbon allotropes aims at studying their mechanical and electronic properties and their potential application as an anode material in lithium-ion batteries (LIB).

Y. Yu investigated the application of graphenylene as an anodic material in LIBs using DFT calculations [7]. The adsorption of Li atoms in graphenylene was reported to be stronger than in pristine graphene, achieving a theoretical capacity of 1116 mA h g⁻¹, which is greater than the graphite capacity. Furthermore, due to the carbon rings C_{12} , diffusion paths were found with low-energy barriers (< 0.9 eV), making it possible to achieve that lithium atoms can be well dispersed on the graphenylene. Recently, T. Qiu et al. [8], reported a theoretical capacity of 837 mA h g⁻¹ and low diffusion barriers (< 0.83 eV) for a new 2D carbon allotrope composed of Quadrangular, Pentagonal, Hexagonal rings and large Tetradecagonal pores (QPHT-graphene) and that exhibit metallic behavior with a significant number of

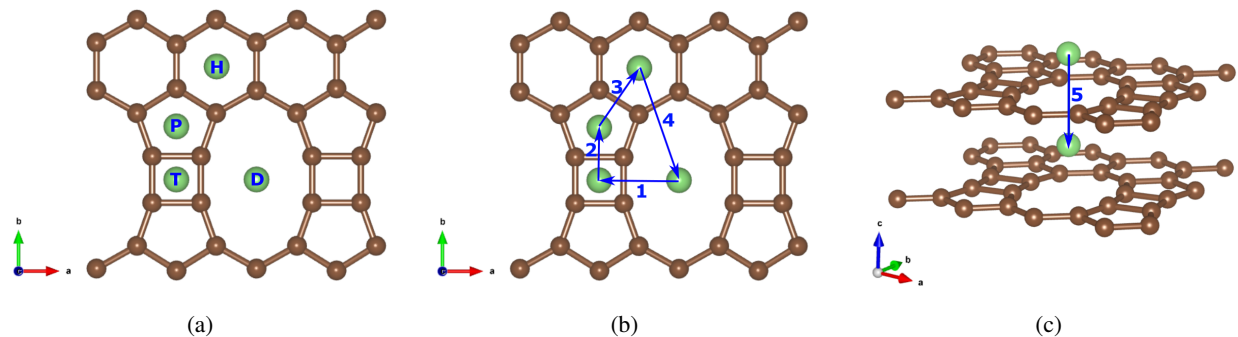


Figure 1: (a) Selected TPDH-gr regions for Li adsorption. (b) Investigated diffusion paths of Lithium ions on the TPDH-gr monolayer. (c) Investigated diffusion path in a TPDH-gr bilayer. These paths were chosen based on minimum energy pathways. See text for discussions.

flat bands near the Fermi level region [8, 3].

The essential requirements for the application of a material as an anode of a LIB are: good thermal stability to not induce structural deformations, high porosity values that are generally satisfied by high-order carbon rings ($C_{>10}$), and high values for electrical conductivity [9]. The vast majority of these new 2D carbon allotropes have good thermal stability, because of strong C-C covalent bonds and high porosity values. However, they can also have large electronic band gap values, negatively influencing their application in LIBs. For example, pentagraphene, formed by C_5 rings, has a theoretical capacity of 1489 mA h g^{-1} , but has a band gap value of $\sim 3.25 \text{ eV}$ [10]. Furthermore, a theoretical capacity of 3916 mA h g^{-1} was reported for twin-graphene, formed by C_6 rings, this value being the largest reported so far [11]. Twin-graphene has semiconductor behavior with a band-gap value of 0.75 eV [12].

Tetra-penta-deca-hexagonal-graphene (TPDH-gr) was recently proposed by D. Bhattacharya and D. Jana [13]. It is a 2D carbon allotrope composed of fully sp^2 carbon atoms arranged in C_4 , C_5 , C_{10} and C_6 rings. TPDH-gr exhibits good mechanical and thermal stability up to 1000K. In addition, TPDH-gr exhibits anisotropic elastic properties due to its ring arrangement topology. The C_4 rings of TPDH-gr were recently reported to be more reactive, capable of adsorbing a larger amount of hydrogen compared to their other rings [14]. Furthermore, Oliveira et al. demonstrated that hydrogenation of TPDH-gr in the C_4 rings also results in anisotropic thermoelectric properties [15].

In this work, the potential application of TPDH-gr as a LIB anode material was investigated using density functional theory (DFT)-based simulations. Through adsorption calculations, a high theoretical capacity of 1116 mA h g^{-1} for TPDH-gr was estimated, and lower diffusion barriers ($< 0.2 \text{ eV}$) were found for Li atoms, comparable to the energy barriers of graphite, which is the most commercially used LIB anode.

2 Computational Methods

The SIESTA software [16, 17] was utilized for all DFT simulations. For all calculations, a 2×1 supercell of TPDH-gr was considered. Periodic boundary conditions were applied to mimic infinitely large systems. A vacuum space of 20 \AA was set to prevent spurious interactions between the layer and its periodic images. Within SIESTA, the Kohn-Sham orbitals were expanded using a double- ζ basis set consisting of numerical pseudoatomic orbitals of finite range, augmented with polarization orbitals. Optimized pseudopotentials and atomic bases from the SIMUNE database [18] were employed with the Perdew-Burker-Ernzerhof (PBE) approximation for the exchange and correlation functional. Furthermore, van der Waals interaction corrections, equivalent to DF1 [19], were incorporated into standard DFT calculations. The Brillouin Zone (BZ) sampling utilized a $5 \times 8 \times 1$ irreducible Monkhorst-Pack (MP) k-point grid [20]. The total energy convergence threshold for each electronic calculation was set at $1 \times 10^{-4} \text{ eV}$. Geometry optimizations were performed using the conjugate gradient (CG) algorithm, ensuring that the magnitude of total forces acting on each ion was minimized to less than 0.01 \AA/eV via ionic position displacements.

We calculated the adsorption energy (E_{ads}) of a lithium atom on TPDH-gr layer using the following equation:

$$E_{\text{ads}} = E_{\text{Li} + \text{TPDH-gr}} - (E_{\text{Li}} + E_{\text{TPDH-gr}}), \quad (1)$$

where $E_{\text{Li} + \text{TPDH-gr}}$ is the total energy of the final configuration of the Li atom adsorption process, while E_{Li} and $E_{\text{TPDH-gr}}$ are the total energy of a gas system of Li and TPDH-gr. An alternative definition of the adsorption energy $E_{\text{ads}}^{\text{bcc}}$ was also considered, where the total energy per atom of lithium in bulk form (bcc) is considered. For both definitions of adsorption energy, negative values indicate that the Li atom is energy favorably adsorbed on TPDH-gr, while positive values indicate no adsorption. As shown in Figure 1a, four adsorption regions (centers of the different rings) were considered: tetragonal (T), pentagonal (P), decagonal (D), and hexagonal (H) sites.

Adsorption calculations were carried out for the ($N = 1, 2, \dots, 6$) Li atoms to find the storage capacity limit of TPDH-gr. For each value of N , 10 random different configurations were considered in which the distances between the lithium atoms were greater than 2.80 \AA which is slightly larger than the molecular distance of Li_2 (2.60 \AA), to prevent Li clustering [21]. These new $E_{\text{ads}}(N)$ are calculated using the following formula:

$$E_{\text{ads}}(N) = E_{N\text{-Li} + \text{TPDH-gr}} - (N E_{\text{Li}} + E_{\text{TPDH-gr}}), \quad (2)$$

where $E_{N\text{-Li} + \text{TPDH-gr}}$ is the total energy of TPDH-gr with N adsorbed Li atoms. Through these calculations, it is possible to determine the maximum number of N Li atoms that can be absorbed, which is where the adsorption energy becomes positive [21]. Therefore, once the value of N has been determined, it is easy to estimate the theoretical capacity of TPDH-gr using the following formula:

$$C = N_{\text{max}} \times \frac{F}{M}, \quad (3)$$

where N_{max} is the maximum number of Li atoms adsorbed on TPDH-gr, $F = 96485.332 \text{ s A/mol}$ is the Faraday constant, and M is the molar mass of the TPDH-gr supercell.

Another important feature of an anode material is the average open-circuit voltage (OCV), which is generally defined as the voltage between the terminals of an electrochemical cell when no current flows through the cell. The OCV can be calculated using the following equation:

$$\text{OCV} = \frac{(E_{\text{TPDH-gr}} + N E_{\text{Li}} - E_{N\text{-Li} + \text{TPDH-gr}})}{N e} \quad (4)$$

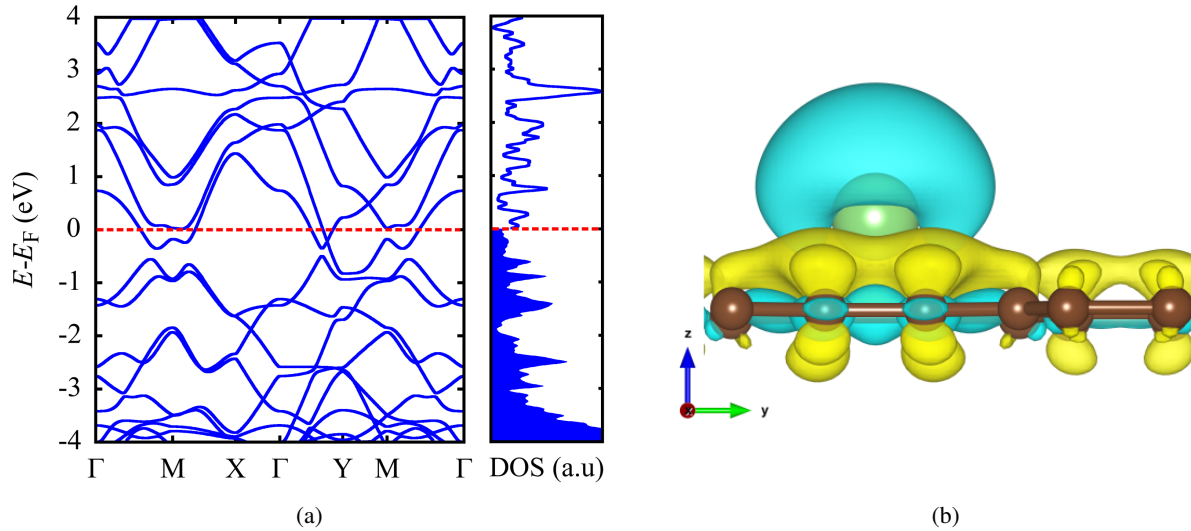


Figure 2: (a) TPDH-gr electronic band structure after the adsorption of Li on the D region. (b) Charge density difference for the adsorption of a single Li atom on TPDH-gr in the D region. The cyan and yellow regions represent the electron losses and gains, respectively. Here, the net charge density difference is defined as the Li-adsorbed TPDH-gr charge density minus the isolated Li atom and TPDH-gr charge density.

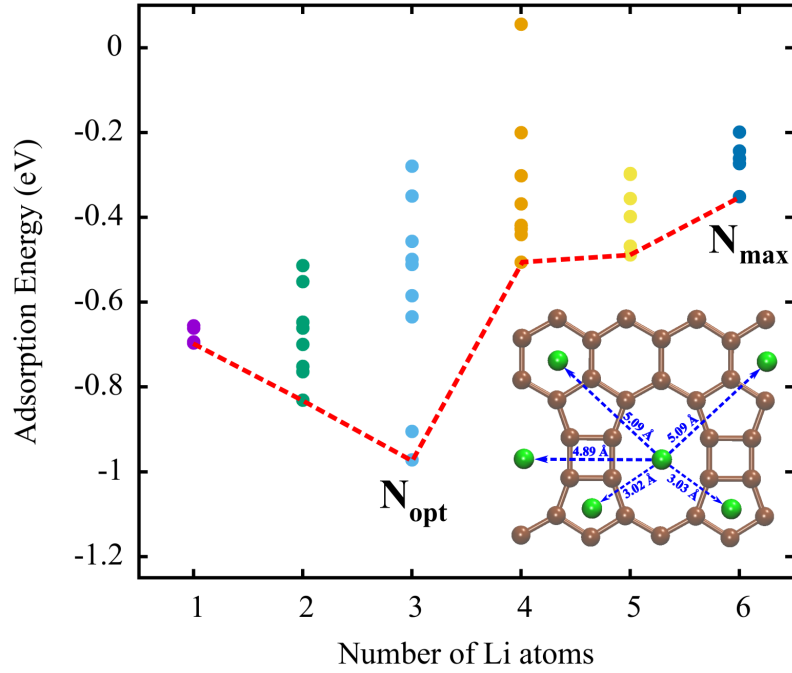


Figure 3: Adsorption energies E_{ads}^{bcc} (eV) as a function of the number N ($N=1,2,\dots,6$) of Li atoms. Inset figure: Configuration of TPDH-gr with $N=6$ Li atoms, showing that the distance between Li atoms is $> 2.80 \text{ \AA}$ to prevent clustering.

where e is the electronic charge of the Lithium-ion. As seen in the previous equation, the OCV is related to the adsorption energy of the lithium atom. Thus, OCV negative values indicate that the adsorption is unfavorable, and the Li atoms will tend to form clusters. In contrast, positive values indicate the possibility of intercalation of Lithium atoms, which further suggests good cycling performance [22, 23, 24].

To characterize Li diffusion on the surface of the TPDH-gr sheet, the minimum energy pathway (MEP) was calculated using nudged elastic band (NEB) calculations [25, 26]. The NEB method was discretized into five images in the configuration space, with fictitious springs connected between the images to prevent them from converging to the same local minima. Initially, images were linearly interpolated between the reactive and product states of the reaction and then optimized using a conjugate gradient method. A climbing image scheme (CI-NEB) [27] was implemented to ensure an accurate determination of the transition state (TS). Five diffusion paths for the Li atom were considered, as shown in Figures 1b and 1c.

3 Results and discussion

In Table 1, we present the values of E_{ads} , E_{ads}^{bcc} , and the perpendicular distance d_{ads} from the Li adsorbed atom to the TPDH-gr layer. The adsorption calculations were carried out for a monolayer and a bilayer of TPDH-gr. These results show that the adsorption of Li on TPDH-gr is thermodynamically favorable, with negative values, and that the sites D and P are the preferential adsorption regions. On the other hand, the values of E_{ads}^{bcc} are also negative values; however, these values are smaller compared to the values of E_{ads} . Additionally, the TPDH-gr bilayer presents adsorption energy slightly higher than that of the monolayer. However, it is also shown that the vdW correction (DF1) has a small effect on the Li adsorption energies and geometries.

In Figure 2a, we present the electronic band structure and the density of electronic states for the final configuration of TPDH-gr with a lithium atom adsorbed in the D region. As can be seen, the TPDH + Li system does not have a band gap because of the intrinsic metallic nature of TPDH-gr. To gain a deeper understanding of the adsorption properties between the Li atom and TPDH-gr, we performed calculations of the charge density differences for the D adsorption region, as shown in Figure 2b. Our analysis revealed that electrons mainly accumulated around the carbon atoms, a

Table 1: Adsorption energy values (E_{ads} and E_{ads}^{bcc}) and final distance (d_{ads}) of the Li atom at the different adsorption regions (D, T, P, and H). For the adsorption process, TPDH-gr monolayers and bilayers were considered. van der Waals corrections (DF1) were also considered. The energies are given in eV, and the distances are in Å

	monolayer				bilayer			
	D	T	P	H	D	T	P	H
E_{ads}	-2.59	-2.55	-2.59	-2.55	-2.65	-2.63	-2.67	-2.63
E_{ads}^{bcc}	-0.70	-0.66	-0.69	-0.66	-0.76	-0.74	-0.78	-0.74
d_{ads}	1.46	1.90	1.82	1.77	1.46	1.86	1.82	1.76
E_{ads} (DF1)	-2.35	-2.30	-2.32	-2.27	-2.44	-2.41	-2.43	-2.39
E_{ads}^{bcc} (DF1)	-0.68	-0.63	-0.65	-0.60	-0.77	-0.74	-0.76	-0.72
d_{ads} (DF1)	1.38	1.91	1.86	1.81	1.49	1.95	1.88	1.83

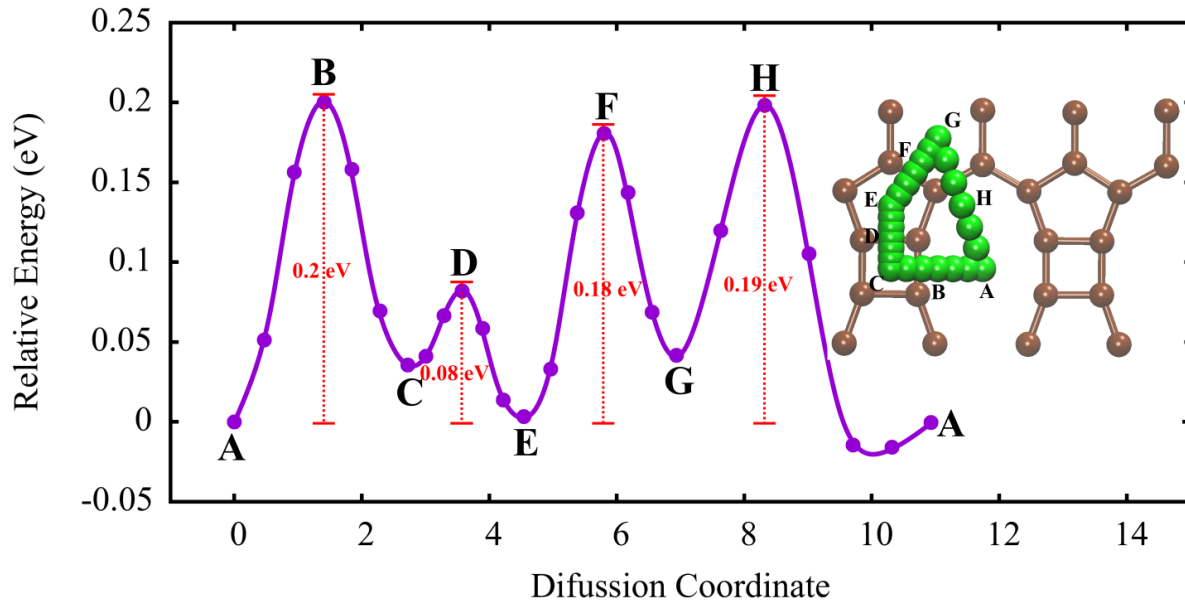


Figure 4: Diffusion energy barriers of the Lithium atom on the surface of TPDH-gr. Inset figure: all intermediate Li images for each diffusion path are shown.

result attributed to the higher electronegativity of carbon compared to lithium.

The adsorption energy values E_{ads}^{bcc} for Li atoms ($N = 1, 2, \dots, 6$) are presented in Figure 3, where we connect the most stable configurations with a dotted line. It is clear that $N=3$ is the optimal amount of Li atoms adsorbed on TPDH-gr, with a maximum value of $E_{ads}^{bcc} \sim -1.0$ eV. In Figure 3, it can also be seen that the maximum amount of Li that can be stored is $N=6$, which only allows a maximum of 7 unique configurations with Li atoms separated by > 2.8 Å (see inset in Figure 3). Considering both TPDH-gr sides, we have $N=12$ as the maximum limit of lithium atoms adsorbed on the TPDH-gr. With these results, it is possible to calculate the theoretical capacity of TPDH-gr (for storage of Li atoms), following equation 3. The C value obtained was 1116 mA h/g. This capacity value is three times larger than the theoretical capacity of graphite ($C = 372$ mA h / g)[28], which is the anode most used in commercial LIB, and is comparable to the theoretical capacity of several 2D carbon allotropes: graphenylene (930 mA h/g), popgraphene (1487 mA h/g) and pentagraphene (1489 mA h/g) [11].

An important factor regarding the charge-discharge performance of a LIB is the diffusion of Li atoms on the surface of TPDH-gr. In Figure 4, the Li diffusion barriers for the four diffusion pathways considered in this study (see Figure 1b) are shown, which were calculated using the NEB method. As can be observed in Figure 4, the energy barriers for Li diffusion have small values, with 0.2 eV being the maximum value for diffusion through pathway 1. Furthermore, the diffusion barriers for pathways 2, 3, and 4 with respect to pathway 1 have the following values: 0.08, 0.18, and 0.19 eV, respectively. The diffusion barrier values for some 2D carbon allotropes are as follows: graphene 0.33 eV, graphite 0.47 eV, biphenylene 0.68 eV, and Pop-graphene 0.58 eV [11]. Therefore, because of the small diffusion barrier value

of TPDH-gr, we can deduce that it could potentially exhibit equal or better performance in the charge and discharge process compared to those of graphene and graphite, which are currently the most widely used anodic materials for LIBs.

For a better understanding of the Li diffusion process on TPDH-gr, we calculated the diffusion coefficients for the four selected pathways. To achieve this, the Arrhenius equation was employed [12]:

$$D_{\text{coeff}}(T) = L^2 \nu_0 \exp\left(-\frac{\Delta E_b}{k_B T}\right) \quad (5)$$

where ΔE_b is the value of the diffusion barriers, L is the length of the diffusion path for the Li atom, T is the absolute temperature in Kelvin units, ν_0 is the vibration frequency, which usually has a value of 10 THz, and k_B is the Boltzmann constant (8.62×10^{-5} eV/K) [12].

In Figure 5, the diffusion coefficient is shown as a function of global temperature for the Li diffusion pathways in TPDH-gr. As observed, the D_{coeff} values at $T=300\text{K}$ vary, with pathways 1 and 3 showing slower Li diffusion. In contrast, the D_{coeff} of Li in pathways 2 and 4 have larger values, indicating faster diffusion in TPDH-gr, even faster than diffusion in graphene ($6 \times 10^{-6} \text{cm}^2/\text{s}$) [12].

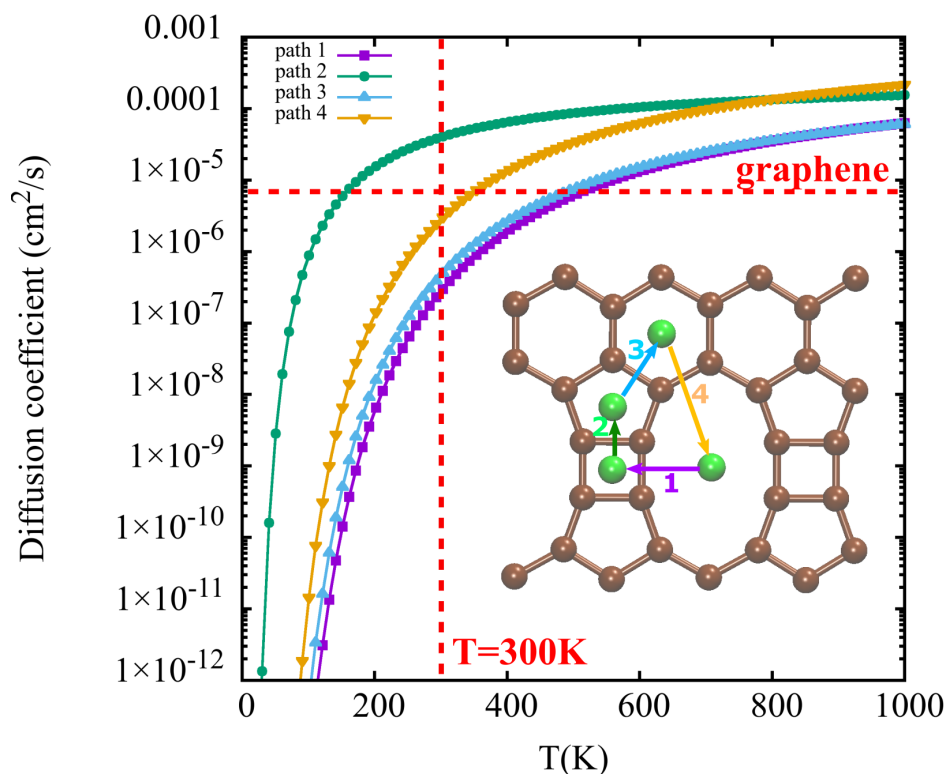


Figure 5: Diffusivity of Li atom over a TPDH-gr as a function of temperature (T). Inset figure: The four diffusion paths of Li on the TPDH-gr are shown.

The Li diffusion barrier for a bilayer TPDH-gr is shown in figure 6a, where the diffusion path corresponds to the migration of the Li atom from the top (region D) to the middle of TPDH-gr, as can be seen in Figure 1c. The diffusion barrier has a value of 0.8 eV, which indicates that Li diffusion occurs more easily on the surface of the TPDH-gr than along the diffusion path between layers. In Figure 6b, the OCV is presented as a function of the number of Li atoms adsorbed in TPDH-gr. As observed in Eq. 4, the OCV correlates with the value of the adsorption energy of the Li atoms. Thus, small OCV values indicate moderate Li adsorption, allowing for easy Li desorption. The average OCV value shown in Figure 6b is 0.29 V, which is very close to the OCV values of other 2D carbon allotropes considered for application as anodes in LIBs: Pop-graphene (0.30 V) and graphenylene (0.34 V) [21].

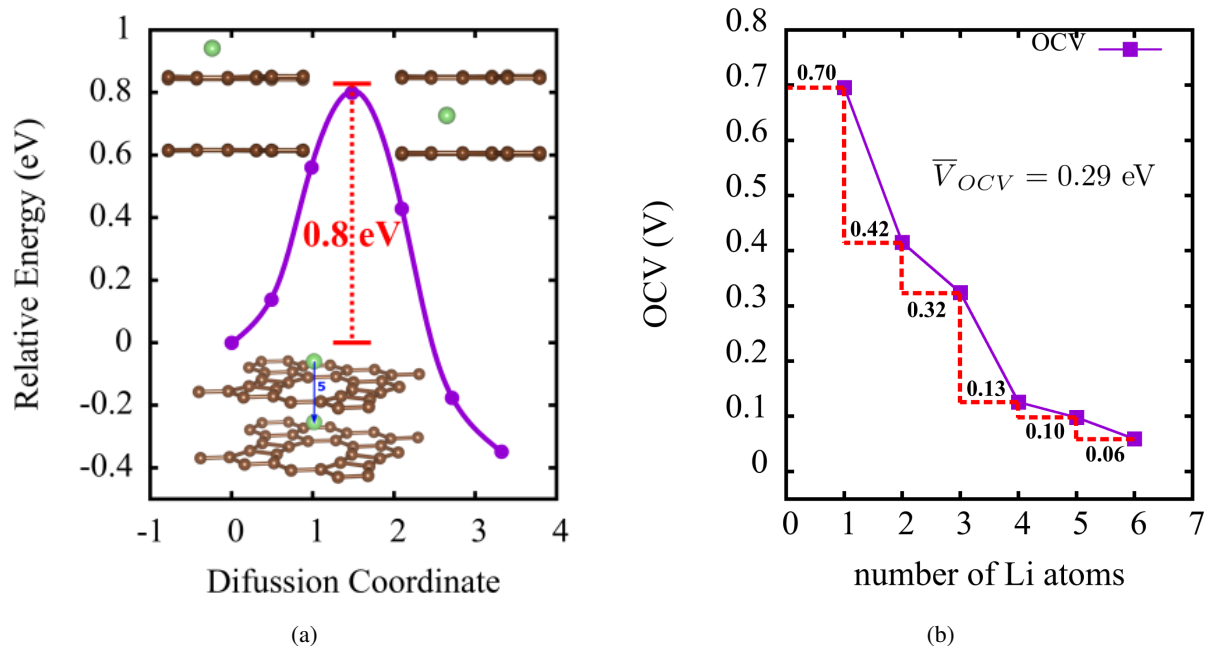


Figure 6: (a) Diffusion barrier of the Lithium atom into a TPDH-gr bilayer. These interlayer diffusions were considered only in the (D) region. (b) Open circuit voltage (OCV) as a function of the number (L) of Li atoms adsorbed on TPDH-gr.

4 Conclusions

In conclusion, we have explored the potential of TPDH-gr as an anode in LIB using DFT-based calculations. Our results indicate that Li-atom adsorption on TPDH-gr is moderate (around 0.70 eV), allowing easy desorption. Additionally, TPDH-gr has a high theoretical capacity of 1116 mAh/gr, making it one of the few 2D carbon allotropes with metallic properties and significant theoretical capacity. Moreover, energy barrier, diffusion coefficient, and OCV calculations show rapid Li-atom diffusion on the surface, stable intercalation of Li atoms, and good performance during the charge and discharge cycles of the LIB. Together, these findings present TPDH-gr as a viable candidate for anode material in LIB.

5 Acknowledgements

JGQ thanks the UFABC Multiuser Computational Center (CCM-UFABC) for the computational resources provided. DSG thanks the Center for Computational Engineering & Sciences (CCES) at Unicamp for financial support through the FAPESP/CEPID Grant 2013/08293-7 and PASA to CNPq (Grant 308428/2022-6). PASA and BI thank to CNPq-INCT (National Institute of Science and Technology on Materials Informatics, grant n. 371610/2023-0).

References

- [1] A. K. Geim and K. S. Novoselov. The rise of graphene. *Nanoscience and Technology: A Collection of Reviews from Nature Journals*, pages 11–19, 2009.
- [2] Tianrong Zhang. *Graphene: From Theory to Applications*. Springer Singapore, Singapore, 2022.
- [3] Susmita Jana, Arka Bandyopadhyay, Sujoy Datta, Debaprem Bhattacharya, and Debnarayan Jana. Emerging properties of carbon based 2D material beyond graphene. *Journal of Physics: Condensed Matter*, 34(5):053001, 2 2022.
- [4] Qi Song, Bing Wang, Ke Deng, Xinliang Feng, Manfred Wagner, Julian D. Gale, Klaus Müllen, and Linjie Zhi. Graphenylene, a unique two-dimensional carbon network with nondelocalized cyclohexatriene units. *J. Mater. Chem. C*, 1(1):38–41, 2013.

- [5] Qitang Fan, Daniel Martin-Jimenez, Daniel Ebeling, Claudio K. Krug, Lea Brechmann, Corinna Kohlmeyer, Gerhard Hilt, Wolfgang Hieringer, André Schirmeisen, and J. Michael Gottfried. Nanoribbons with Nonalternant Topology from Fusion of Polyazulene: Carbon Allotropes beyond Graphene. *Journal of the American Chemical Society*, 141(44):17713–17720, 2019.
- [6] Wei Zhang, Changchun Chai, Qingyang Fan, Yanxing Song, and Yintang Yang. Two-dimensional carbon allotropes with tunable direct band gaps and high carrier mobility. *Applied Surface Science*, 537(July 2020):147885, 2021.
- [7] Yang Xin Yu. Graphenylene: A promising anode material for lithium-ion batteries with high mobility and storage. *Journal of Materials Chemistry A*, 1(43):13559–13566, 2013.
- [8] Tian Chong Qiu, Zhi Gang Shao, Cang Long Wang, and Lei Yang. QPHT graphene as a high-performance lithium ion battery anode materials with low diffusion barrier and high capacity. *Physics Letters, Section A: General, Atomic and Solid State Physics*, 456:128549, 2022.
- [9] Jianmin Ma, Yutao Li, Nicholas S. Grundish, John B. Goodenough, Yuhui Chen, Limin Guo, Zhangquan Peng, Xiaoqun Qi, Fengyi Yang, Long Qie, Chang An Wang, Bing Huang, Zeya Huang, Linhui Chen, Dawei Su, Guoxiu Wang, Xinwen Peng, Zehong Chen, Junliang Yang, Shiman He, Xu Zhang, Haijun Yu, Chaopeng Fu, Min Jiang, Wenzhuo Deng, Chuan Fu Sun, Qingguang Pan, Yongbing Tang, Xianfeng Li, Xiulei Ji, Fang Wan, Zhiqiang Niu, Fang Lian, Caiyun Wang, Gordon G. Wallace, Min Fan, Qinghai Meng, Sen Xin, Yu Guo Guo, and Li Jun Wan. The 2021 battery technology roadmap. *Journal of Physics D: Applied Physics*, 54(18), 2021.
- [10] Bo Xiao, Yan-chun Li, Xue-fang Yu, and Jian-bo Cheng. Penta-graphene: A Promising Anode Material as the Li/Na-Ion Battery with Both Extremely High Theoretical Capacity and Fast Charge/Discharge Rate. *ACS Applied Materials & Interfaces*, 8(51):35342–35352, 12 2016.
- [11] A Rajkamal and Ranjit Thapa. Carbon Allotropes as Anode Material for Lithium-Ion Batteries. *Advanced Materials Technologies*, 4(10):1–20, 10 2019.
- [12] Shuli Gao, Elyas Abduryim, Changcheng Chen, Chao Dong, Xiaoning Guan, Shuangna Guo, Yue Kuai, Ge Wu, Wen Chen, and Pengfei Lu. Twin-Graphene: A Promising Anode Material for Lithium-Ion Batteries with Ultrahigh Specific Capacity. *Journal of Physical Chemistry C*, 127(29):14065–14074, 2023.
- [13] Debaprem Bhattacharya and Debnarayan Jana. TPDH-graphene: A new two dimensional metallic carbon with NDR behaviour of its one dimensional derivatives. *Physica E: Low-Dimensional Systems and Nanostructures*, 127(November 2020):114569, 2021.
- [14] Caique C Oliveira, Matheus Medina, Douglas S Galvao, and Pedro A. S. Autreto. Tetra-penta-deca-hexagonal-graphene (TPDH-graphene) hydrogenation patterns: dynamics and electronic structure. *Physical Chemistry Chemical Physics*, 25(18):13088–13093, 2023.
- [15] Caique C. Oliveira, Douglas S. Galvão, and Pedro A.S. Autreto. Selective Hydrogenation Promotes the Anisotropic Thermoelectric Properties of TPDH-Graphene. *Journal of Physical Chemistry C*, 2024.
- [16] José M. Soler, Emilio Artacho, Julian D. Gale, Alberto García, Javier Junquera, Pablo Ordejón, and Daniel Sánchez-Portal. The SIESTA method for ab initio order- N materials simulation. *Journal of Physics: Condensed Matter*, 14(11):2745–2779, 3 2002.
- [17] Alberto García, Nick Papior, Arsalan Akhtar, Emilio Artacho, Volker Blum, Emanuele Bosoni, Pedro Brandimarte, Mads Brandbyge, J. I. Cerdá, Fabiano Corsetti, Ramón Cuadrado, Vladimir Dikan, Jaime Ferrer, Julian Gale, Pablo García-Fernández, V. M. García-Suárez, Sandra García, Georg Huhs, Sergio Illera, Richard Korytár, Peter Koval, Irina Lebedeva, Lin Lin, Pablo López-Tarifa, Sara G. Mayo, Stephan Mohr, Pablo Ordejón, Andrei Postnikov, Yann Pouillon, Miguel Pruneda, Roberto Robles, Daniel Sánchez-Portal, Jose M. Soler, Rafi Ullah, Victor Wen Zhe Yu, and Javier Junquera. Siesta: Recent developments and applications. *Journal of Chemical Physics*, 152(20), 2020.
- [18] J Oroya, A Martín, M Callejo, M García-Mota, and F Marches. Pseudopotential and Numerical Atomic Orbitals Basis Dataset, provided by SIMUNE Atomistics (www.simuneatomistics.com).
- [19] M. Dion, H. Rydberg, E. Schröder, D. C. Langreth, and B. I. Lundqvist. Van der Waals density functional for general geometries. *Physical Review Letters*, 92(24):22–25, 2004.
- [20] Hendrik J. Monkhorst and James D. Pack. Special points for Brillouin-zone integrations. *Physical Review B*, 13(12):5188–5192, 6 1976.
- [21] Saif Ullah, Marcos G. Menezes, and Alexander M. Silva. Theoretical characterization of tolanene: A new 2D sp-sp² hybridized carbon allotrope. *Carbon*, 217(September 2023):118618, 2024.
- [22] Qiu He, Bin Yu, Zhaohuai Li, and Yan Zhao. Density Functional Theory for Battery Materials. *Energy & Environmental Materials*, 2(4):264–279, 2019.

- [23] Gladys W. King'ori, Cecil N.M. Ouma, George O. Amolo, and Nicholas W. Makau. Ab initio insights into Graphene-Zirconium disulfide/diselenide heterostructure as electrode material for alkali-ion batteries. *Surfaces and Interfaces*, 24(December 2020), 2021.
- [24] Bruno Ipaves, João F. Justo, and Lucy V.C. Assali. Aluminum functionalized few-layer silicene as anode material for alkali metal ion batteries. *Molecular Systems Design and Engineering*, 8(3):379–387, 2022.
- [25] Daniel Sheppard, Rye Terrell, and Graeme Henkelman. Optimization methods for finding minimum energy paths. *Journal of Chemical Physics*, 128(13), 2008.
- [26] Søren Smidstrup, Andreas Pedersen, Kurt Stokbro, and Hannes Jónsson. Improved initial guess for minimum energy path calculations. *Journal of Chemical Physics*, 140(21):0–6, 2014.
- [27] Graeme Henkelman, Blas P. Uberuaga, and Hannes Jónsson. Climbing image nudged elastic band method for finding saddle points and minimum energy paths. *Journal of Chemical Physics*, 113(22):9901–9904, 2000.
- [28] Jakob Asenbauer, Tobias Eisenmann, Matthias Kuenzel, Arefeh Kazzazi, Zhen Chen, and Dominic Bresser. The success story of graphite as a lithium-ion anode material—fundamentals, remaining challenges, and recent developments including silicon (oxide) composites. *Sustainable Energy & Fuels*, 4(11):5387–5416, 2020.